Negative refraction in two-dimensional photonic crystals: Role of lattice orientation and interface termination

Alejandro Martínez* and Javier Martí
Valencia Nanophotonics Technology Center, Universidad Politécnica de Valencia, Campus del Camino de Vera, 46022 Valencia, Spain
(Received 24 January 2005; revised manuscript received 15 March 2005; published 28 June 2005)

Negative refraction at the interface between air and a two-dimensional photonic crystal is analyzed at frequencies corresponding to the second photonic band. In the study, several lattice orientations and interface terminations of a photonic crystal slab are considered. Finite-difference time-domain simulations are carried out and compared to an analysis using equifrequency contours. The results show that negative refraction and the resulting focusing effects occur under certain conditions but the photonic crystal does not behave in general as an effective refractive medium because the propagation inside the crystal strongly depends on the interface termination. In addition, the Goos-Hänchen effect must be taken into account to obtain the effective index of refraction for a finite photonic crystal slab when negative refraction occurs.

DOI: 10.1103/PhysRevB.71.235115 PACS number(s): 78.20.Ci, 42.70.Qs, 41.20.Jb, 42.25.Gy

I. INTRODUCTION

Photonic crystals (PhCs)[1,2] are periodic arrangements of scatterers in which electromagnetic (EM) propagation in the form of Bloch waves is governed by the photonic band structure.[3] The propagation of EM waves inside a PhC is a consequence of the multiple diffraction through the strongly modulated periodic lattice of dielectric scatterers, which can give rise to extraordinary physical phenomena such as the so-called negative refraction. Notomi[3] showed that PhCs can mimic the behavior of dielectric materials with an effective index of refraction in certain spectral regions for which the so-called equifrequency contours (EFCs) become rounded, despite the fact that the underlying physical phenomenon is not actually refraction. When an EM wave propagating through air (or another effective dielectric medium) impinges on a PhC interface, the direction of propagation of the EM radiation inside the PhC can be obtained by analyzing the EFCs of both media and taking into account the conservation of the wave vector component parallel to the interface.[4] If a certain rounded PhC EFC shrinks with increasing frequency then the group velocity vector points inwards and a phenomenon that resembles negative refraction can be expected at the interface between the PhC and air.[3]

Negative refraction in PhCs was observed experimentally at optical frequencies by Kosaka and co-workers[4] and, afterwards, it has been the subject of intense theoretical studies, numerical simulations, and experimental measurements.[3,5–10] It should be pointed out that all these works have been focused on two-dimensional (2D) PhCs as they can be analyzed in a more flexible and straightforward way than their three-dimensional counterparts. One of the most interesting applications of negative refraction is the realization of flat lenses[11] that can partly overcome the diffraction limit.[12]

In general, negative refraction in 2D PhCs occurs under two conditions:[7] (i) at frequencies in which the propagation is forbidden along one of the main symmetry directions (partial gap) and allowed in the other one;[8] and (ii) at frequencies in which the EFCs of the PhC have a rounded shape whose radius diminishes with increasing frequency so the wave vector and the group velocity are antiparallel.[3] The first case is common for frequencies in the first photonic band near the band gap. The second case takes place at higher photonic bands. In this paper, we will consider the second photonic band for which at certain frequencies the condition explained in (ii) is satisfied. The mechanism giving rise to negative refraction is well different in both cases. Negative refraction in the first band occurs due to the anisotropy of the material but the effective index is positive. Moreover, recent studies by Ye and co-workers[13,14] suggest that a collimation or self-guiding effect instead of a true refraction is the phenomenon that takes place, as the radiation inside the PhCs tends to bend away from the forbidden direction. For example, Snell's law is not met at the air-PhC interface in this case. This means that this phenomenon can be classified as negative deflection of the beam, but not as a true negative refraction. However, an effective negative index of refraction n_{eff} can be associated to a PhC in the frequency region of the second photonic band (also in higher photonic bands[7,10]) where the EFCs become rounded as in conventional isotropic dielectrics, and their radii shrinks with increasing frequency so, since the propagation direction is given by the group velocity that is normal to the EFC, the energy flow is antiparallel to the wave vector.[3] In principle, in this region the PhC should behave (in terms of refraction at the interfaces) as a left-handed medium[11] that satisfies the Snell's law but with a negative index of refraction.[7]

In this work, the negative refraction phenomenon at frequencies corresponding to the second photonic band of a 2D square PhC is investigated by means of an EFC analysis and finite-difference time-domain (FDTD) simulations. An EM Gaussian beam that resembles a plane wave impinges on a PhC slab with input and output interfaces to air. Inside the slab, the lattice orientation is changed and different directions as well as slab terminations are considered: interface along ΓX, along MM and forming angles of 26.56° and 30° with respect to both ΓX and ΓM directions. The reason for these changes in the lattice orientation is to verify if the PhC behaves as an effective refractive medium with $n_{\text{eff}}<0$ in agreement with the behavior that can be expected from the

rounded shape of the EFCs. In principle, if the PhC behaves as an effective medium the orientation of the lattice as well as the structure of the slab termination should not have influence on the EM wave propagation. We will show that the periodicity of the interface plays a fundamental role on the behavior of the PhC as a negative refractive medium. The conditions to be met by the PhC in order to resemble a negative refraction behavior will be discussed. Under these conditions, the PhC slab can focus the input radiation and behaves like a flat lens as predicted for left-handed media. In addition, the differences between the effective index calculated for an infinite PhC and for a PhC slab will be explained.

The paper is structured as follows: in Sec. II the PhC as well as the system used to study the refractive behavior are described. In Sec. III the analysis for the four lattice orientations under consideration is carried out. Section IV presents a discussion on the obtained results and the effect of these results on the PhC focusing properties. Finally, some conclusions are given in Sec. V.

II. DESCRIPTION OF THE PHOTONIC CRYSTAL AND THE REFRACTION SCENARIO UNDER STUDY

In our study, we consider a square lattice of circular air holes in a dielectric background with the following parameters: the radius of the holes is $0.35a$, a being the lattice constant, and the permittivity of the dielectric is $\varepsilon=12$. Only TE modes (magnetic field parallel to the axis of the holes) are considered. The band structure of this PhC can be found in Refs. 8 and 14. Figure 1(a) depicts several EFCs at different frequencies of the second photonic band and for the first Brillouin zone of the square lattice [see top inset in Fig. 1(b)]. The EFCs have been obtained by use of the plane wave expansion (PWE) method. It should be mentioned that the unit cell shown in Fig. 1(a) is actually replicated over the whole reciprocal space since we are considering a 2D periodic system (this question will be considered in depth in the following section). Frequencies are represented in normalized units, fa/c, f being the absolute frequency and c the light speed in vacuum. From Fig. 1(a) it can be noted that EFCs shrink when frequency increases, so the group velocity, defined as $\vec{v}_g=2\pi\nabla_{\vec{k}}f$, is negative and, from the conservation of the parallel component of the wave vector at the interface and taking into account causality considerations, the component of the wave vector normal to the interface should reverse its sign when passing from air to the PhC and again from the PhC to air.[3,11] This means that at interfaces the beam will be deflected to the same side of the normal to the interfaces, resembling a negative refraction behavior. We can also note that the shape of the EFCs is squarelike for low frequencies and becomes rounder and rounder with increasing frequencies. It should be mentioned that when the shape is squarelike and under certain conditions the PhC can guide incident waves along the ΓX direction regardless of the incident angle, so the PhC acts as a collimator.[15]

In a 2D PhC, n_{eff} can be obtained following the procedure described in Ref. 7. Figure 1(b) depicts n_{eff} for the second photonic band along the two main directions of symmetry

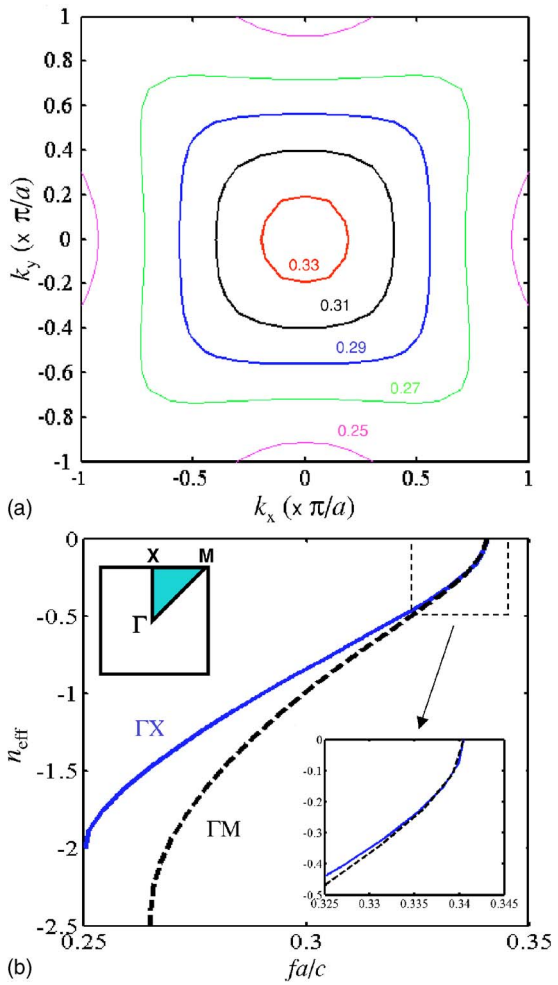

FIG. 1. (Color online) (a) EFCs of the proposed 2D PhC for several frequencies ($fa/c=0.25,0.27,0.29,0.31,0.33$) in the second photonic band; (b) effective refractive index n_{eff} for the two main symmetry directions (ΓX and ΓM) in the second photonic band. Top inset: first Brillouin zone of the square lattice. Bottom inset: detailed view of n_{eff} around $fa/c=0.33$.

(ΓM and ΓX). At low frequencies n_{eff} is quite different for ΓM and ΓX directions (square-shaped EFCs) but it tends to be equal with increasing frequencies (rounded EFCs), as shown in the bottom inset, in which a detailed view of n_{eff} in the second band high frequency region is depicted. It can be assumed that the index is equal for both directions at frequencies above 0.32, so in this range the PhC should behave, in principle, as an effective medium with $n_{\text{eff}}<0$.[3]

The refractive behavior is analyzed by means of 2D FDTD simulations[16] with perfectly matched layer boundary conditions.[17] An EFC analysis over the 2D reciprocal space will be carried out previously to predict the behavior of the EM wave propagation inside the slab. We consider a rectangular slab of thickness L much larger than the free-space wavelength λ, as depicted in Fig. 2(a). This scenario is similar to that employed in experimental setup in Ref. 6 and has been proven to be well suited to study negative refraction. The beam propagating inside the PhC forms an angle ϕ_r with respect to the normal to the interfaces. The angle ϕ_r can be calculated from the lateral shift d, which is obtained from the

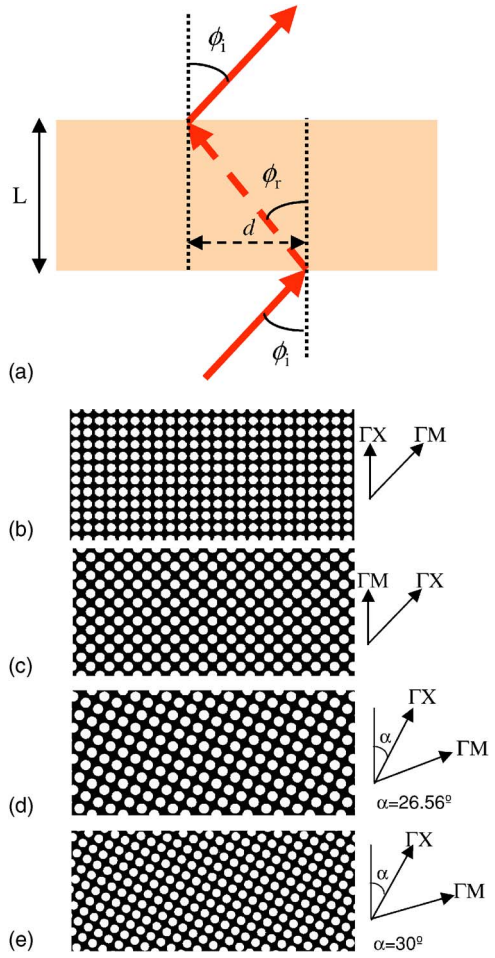

FIG. 2. (Color online) (a) Scheme of the system used to study the negative refractive index behavior: a Gaussian wave propagates through air and impinges on a PhC slab with thickness L forming an angle ϕ_i with the normal to the interface; inside the PhC, the beam propagates forming an angle ϕ_r with respect to the normal and is shifted a distance $d=L\tan(\phi_r)$ to the same side of the normal; at the output interface the wave forms an angle ϕ_i with the normal, assuming that the slab has a refractive behavior. Different lattice orientations inside the slab as well as slab terminations are used in the simulations: (b) orientation 1, the interface is normal to ΓX; (c) orientation 2, the interface is normal to ΓM; (d) orientation 3, the normal to the interface forms an angle $\alpha=26.56°$ with respect to ΓX; (e) orientation 4, the normal to the interface forms an angle $\alpha=30°$ with respect to ΓX. The surface termination for both input and output interfaces correspond to those employed in the FDTD simulations.

input and output beams propagating through air. It is assumed that the beam is deflected in the negative direction. Four different orientations (and slab terminations) of the periodic lattice inside the slab are considered, as shown in Figs. 2(b), 2(c), 2(d), and 2(e), which hereinafter will be referred to as orientation 1 (interface normal to ΓX), 2 (interface normal to ΓM), 3 (interface normal to a line forming an angle $\alpha=26.56°$ with the ΓX direction), and 4 (interface normal to a line forming an angle $\alpha=30°$ with the ΓX direction). For orientations 1–3 the slab termination is periodic but for orientation 4 the angle α has been properly chosen to avoid periodicity along the interface. The incident wave is a Gaussian beam with frequency $fa/c=0.33$ [the corresponding EFC is rounded and $n_{\text{eff}}=-0.36$ from Fig. 1(b)] and a transverse width $15a$ that is much larger than λ at the chosen frequency, so we can assume that a unique wave vector impinges onto the PhC surface (plane wave behavior). The transversal width is also large enough so that the input wave feels the periodicity of the interface.

III. ANALYSIS OF THE NEGATIVE REFRACTIVE BEHAVIOR

A. PhC slab with orientation 1

First we consider the slab with orientation 1 as shown in Fig. 2(b). When the wave propagating through air impinges on the interface of the 2D PhC slab, a Bloch mode is excited inside the PhC[18] if the interface is properly chosen, as we will see below. This Bloch mode is comprised of a set of plane waves whose wave vectors are related by an integral number of reciprocal lattice vectors that can be defined as $\vec{G}_x=(2\pi/a)\hat{x}$ and $\vec{G}_y=(2\pi/a)\hat{y}$ for the square lattice. The component of the magnetic field of the Bloch wave parallel to the rod axis can be written as follows:

$$H_z=\sum_{m,n} H_{m,n}\exp[j(\vec{k}_0+m\vec{G}_x+n\vec{G}_y)\cdot\vec{r}], \tag{1}$$

$\vec{k}_0$ being the fundamental wave vector of the Bloch mode (this is, the wave vector inside the first Brillouin zone), $H_{m,n}$ the field amplitude of the mn-plane wave forming the Bloch mode and $\vec{r}$ the position vector on the 2D space. The direction of propagation (angle ϕ_r) of this Bloch mode will be given by the group velocity that is normal to the EFC at a given frequency. At the interface the following condition must be satisfied:[19]

$$k_{r\|}=k_{i\|}+\frac{2\pi m}{P}, \tag{2}$$

where $k_{i\|}$ and $k_{r\|}$ are, respectively, the components parallel to the interface of the incident and refracted wave vectors [$k_{i\|}=|\vec{k}_i|\sin(\phi_i)$ and $|\vec{k}_i|=2\pi f/c$], P is the periodicity of the interface, which is a for orientation 1, and m is an integer. It should be mentioned that $k_{r\|}$ may be the wave vector component parallel to the interface of any plane wave forming a Bloch wave that propagates inside the PhC. The direction of propagation inside the PhC slab can be obtained by means of an EFC diagram as that shown in Fig. 3 for orientation 1. As stated above, the full reciprocal space must be considered because the PhC has a 2D periodicity. For the sake of simplicity, in Fig. 3 only nine reciprocal unit cells are shown but as we will see this is sufficient in our study. Solid blue and dotted red circles stand for the EFCs of the PhC and air at $fa/c=0.33$, respectively. The incident wave vector $\vec{k}_i$ is represented as a red arrow (see also scheme at the bottom of Fig. 3). Vertical bold dashed lines are normal to the interface and spaced $2\pi/P$ and represent condition (2). Each time that a vertical line intersects a PhC EFC, a wave vector that forms part of a whole Bloch wave [see Eq. (1)] is defined. It can be

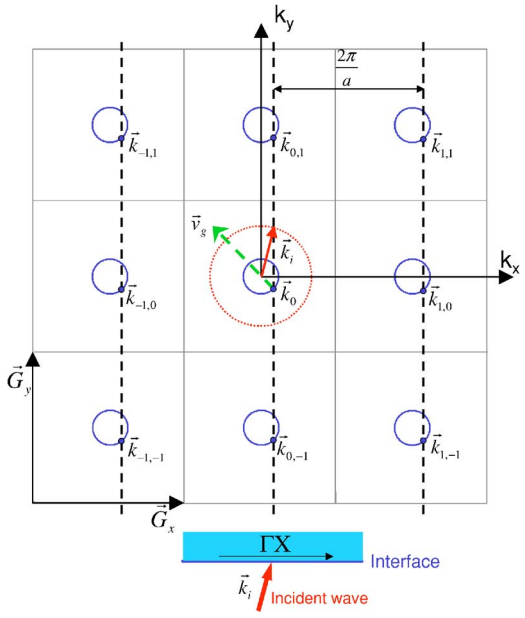

FIG. 3. (Color online) EFC diagram of refraction at the air-PhC interface for orientation 1 and $fa/c=0.33$. Nine reciprocal unit cells are shown. Blue solid and red dotted circles stand for the EFCs inside the PhC and in air, respectively. Vertical dashed lines (spaced $2\pi/a$) represent the conservation of the parallel component of the wave vectors. The wave vector of the incident waves is given by $\vec{k}_i$. The propagation direction inside the PhC is given by $\vec{v}_g$ (green dashed arrow). Bottom: scheme of the interface for orientation 1.

noted that each PhC EFC is intersected at two different points. However, to preserve causality only the lower intersection points are considered because the group velocity points inwards, which in this case (see Fig. 3) is away from the EM source. In Fig. 3 we can see that nine different wave vectors (in the whole reciprocal space, there will be infinite wave vectors) are solutions of Eq. (2). However, each one of these wave vectors are related to each other since $\vec{k}_{m,n}=\vec{k}_0+m\vec{G}_x+n\vec{G}_y$, for m, $n=-1$, 0, and 1. This would occur even if the whole reciprocal space is considered, owing to the periodicity of the interface and the symmetry of the structure. This means that all the wave vectors correspond to a unique Bloch mode that will propagate in the direction given by the vector $\vec{v}_g$ (dashed green arrow in Fig. 3). Since $\vec{v}_g$ and $\vec{k}_0$ are antiparallel and a unique Bloch mode is excited, we can consider that the EM wave is negatively refracted at the interface.

This predicted behavior can be tested by means of FDTD simulations of the system depicted in Fig. 2(a). Figures 4(a), 4(b), 4(c), 4(d), and 4(e) show the magnetic field distribution in the system depicted in Fig. 2(a) for orientation 1, $fa/c=0.33$ and $\phi_i=2.5°$, 7.5°, 12.5°, 17.5°, and 22.5°, respectively. It can be observed from the field distributions in Fig. 4 that the field is negatively deflected at the input interface as expected from the previous EFC study. For large incident angles the angular spreading of the beam inside the PhC is quite large. This occurs because inside the PhC $|n_{\text{eff}}|<1$ so the beam spreads out more rapidly than in air as the effective wavelength is larger for a same initial width of the beam. This spreading could be reduced by using wider beams which would require a larger FDTD simulation region and, consequently, a larger computation time.

The relationship between ϕ_i and ϕ_r is given in Fig. 5. Open circles stand for the estimated values from the field distributions of FDTD simulations and the solid line shows ϕ_r obtained applying the Snell's law with $n_{\text{eff}}=-0.534$ that is the average value of the obtained n_{eff}. It can be observed that the deflection of the beam follows approximately the Snell's law so the underlying phenomenon mimics refraction, although it is an effect of the band structure of the PhC. This phenomenon does not occur for lower frequencies in the second photonic band, for which the beam is also deflected negatively but the refracted beam does not follow the Snell's law. From these results, it can be stated that for orientation 1 and frequencies in which the EFC are rounded, the PhC resembles an effective refractive medium with a certain effective index of refraction n_{eff}. However, in Fig. 1(b) we can observe that n_{eff} obtained from the band diagram (infinite PhC) is about -0.36 for $fa/c=0.33$, which is different to the value of -0.534 obtained from FDTD simulations. It is clear that since both results are obtained by means of different numerical methods a slight difference between the calculated values can be expected. For example, if we assume that the calculation of the photonic bands by means of the PWE method produces a 1.5% downward shift on the obtained frequencies, then the effective index at $fa/c=0.33$ would be $n_{\text{eff}}=-0.44$, which is closer but still far from the to the value obtained from FDTD simulations (-0.534). Thus, we think that the difference is too large to be caused uniquely by a mismatch between the employed numerical methods and there may be another mechanism that could contribute to this observed difference. In our opinion, this additional contribution to the difference between the estimated n_{eff} in each case can arise from the finiteness of the system under study [see Fig. 2(a)]: waves are not really refracted and reflected at the interfaces, but at planes slightly shifted upwards and downwards the interfaces, which produces a lateral displacement of the refracted and reflected fields due to the excitation of evanescent fields at the interfaces that are not considered in the infinite PhC analysis. This phenomenon has been recently predicted to occur in PhCs as a generalized version of the Goos-Hänchen effect.[20]

To evaluate the effect of the Goos-Hänchen shift in obtaining both ϕ_r and n_{eff}, we realized a series of FDTD simulations in which the PhC slab thickness L was varied from $2a$ to $28a$ in $2a$ steps. Only integral multiples of a were chosen for L to ensure that both input and output interfaces are equal and the slab terminations are as depicted in Fig. 2(b). The incident angle was chosen $\phi_i=10°$. Figures 6(a) and 6(b) show, respectively, the obtained values of ϕ_r and n_{eff} with respect to L. Open circles stand for the values obtained from FDTD simulations and the parallel solid line is the value obtained from the PWE method, which assumes an infinite PhC. The possible deviation to a slightly lower effective negative index introduced by the PWE and commented above is not considered. It is worth noting the resemblance between Figs. 6(a) and 4 in Ref. 20, which lead us to conclude that the Goos-Hänchen effect must be taken into account when analyzing refractive effects in PhC slabs. In Ref.

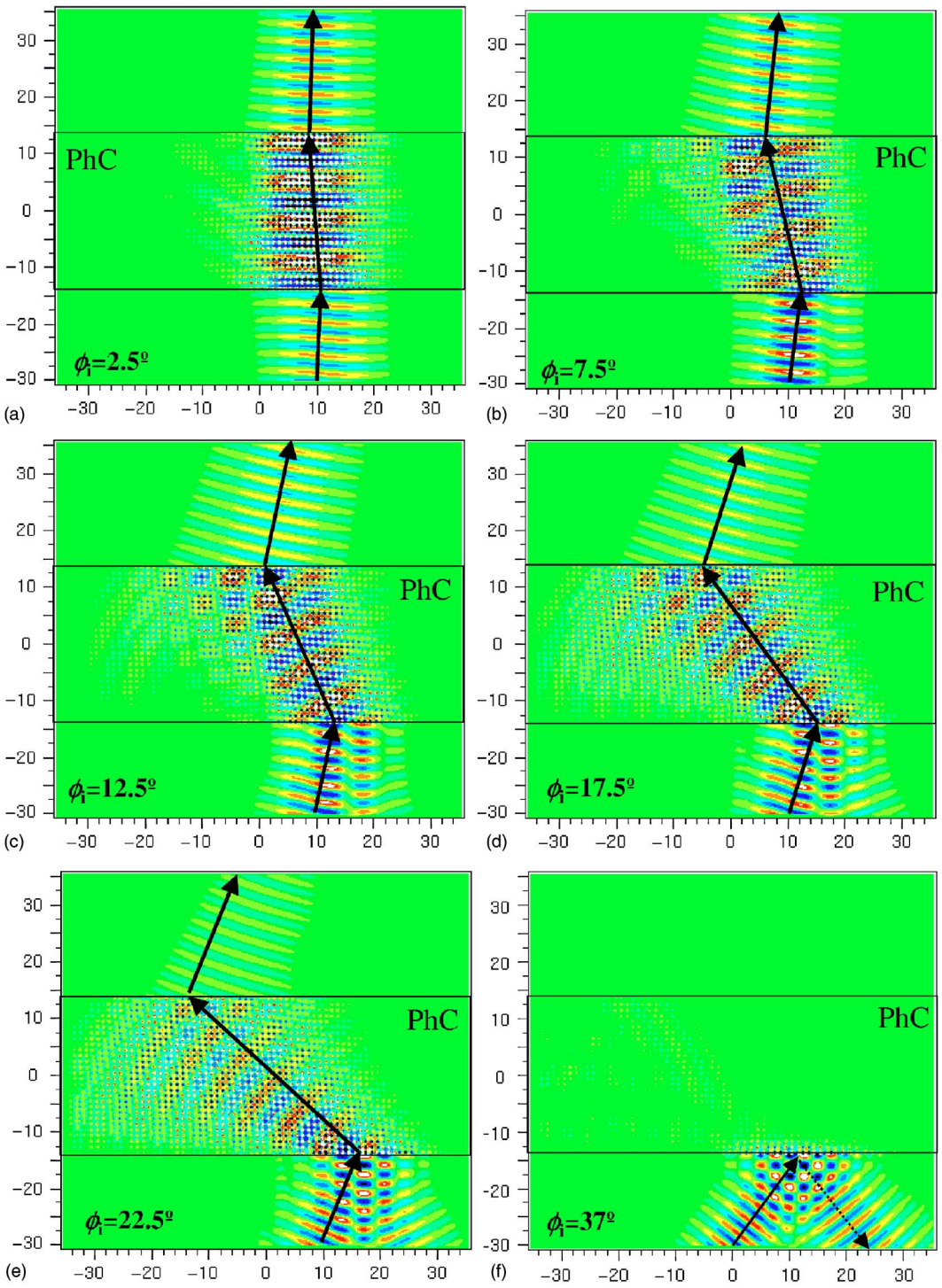

FIG. 4. (Color online) Distribution of the magnetic field parallel to the rods (FDTD simulations) for orientation 1 and $fa/c=0.33$. The incident angle ϕ_i is highlighted in each snapshot. The boundaries of the PhC slab are defined by the rectangle. The width of the input beam is $15a$. Arrows highlight the direction of the energy of the incident wave, the wave inside the slab and the output wave. Red, green, and blue colors stand for positive, zero, and negative amplitude of the propagating field. The snapshots have been obtained after a simulation time of $ct/a=300$.

20 the refracted angle for the finite structure is higher than that for the infinite PhC because refraction is positive. In our case, refraction is negative and the refracted angle is higher for the infinite PhC. This can be explained by considering that the shift of the refraction interfaces is positive regardless of the sign of the refractive index. It is also interesting to note that n_{eff} tends to be constant (about -0.56) for $L>12a$ but it has an oscillating behavior for small L. This oscillating behavior can arise from Fabry-Pérot-like reflections at the interfaces that can affect the beam outside of the slab when

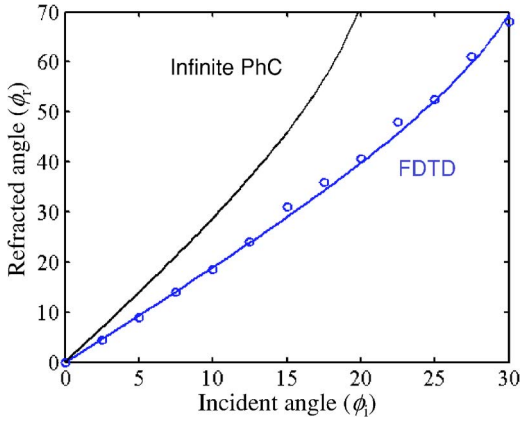

FIG. 5. (Color online) Refracted angle ϕ_r as a function of the incident angle ϕ_i for orientation 1 and $fa/c=0.33$. Blue open circles: values obtained from FDTD simulations; blue solid curve: Snell's law assuming $n_{eff}=-0.534$ (mean of the obtained values); black dashed curve: Snell's law assuming $n_{eff}=-0.36$ (calculated for an infinite PhC).

the value of L is small enough. This assumption is in agreement with the fact that the oscillation occurs around a mean value similar to that estimated for higher values of L. Anyway, we can conclude that although n_{eff} for the real finite system cannot be obtained without considering the presence of evanescent waves that modify the EFCs for the case of a finite system, the PhC slab follows the Snell's law with a negative n_{eff}.

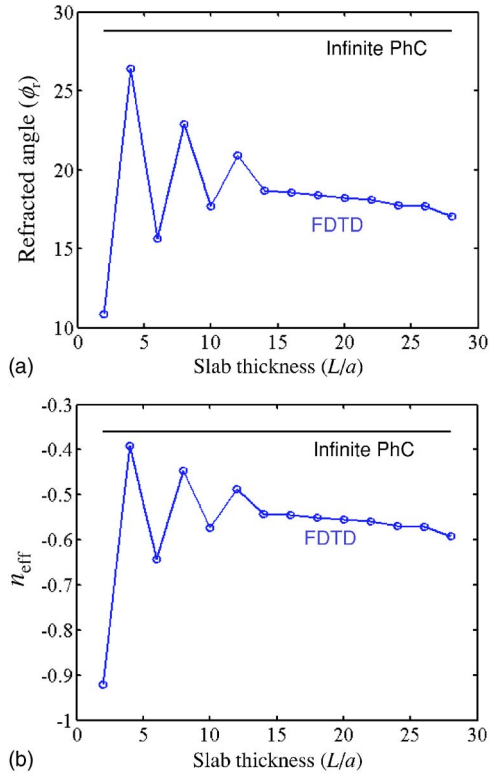

FIG. 6. (Color online) (a) Refracted angle ϕ_r and (b) effective index of refraction n_{eff} as a function of the slab thickness L for orientation 1, $\phi_i=10°$ and $fa/c=0.33$. Blue open circles: values obtained from FDTD simulations; black solid line: value obtained using the PWE method (infinite PhC).

Since the radius of the EFC for $fa/c=0.33$ is much smaller than the radius of the air EFC, an external plane wave cannot enter the PhC for all possible incident angles. Theoretically, for $\phi_i > \phi_{max}=a\sin(|n_{eff}|)=32.7°$ the wave cannot propagate inside the PhC since the vertical dashed lines that define the conservation of the wave vector parallel to the interface does not intersect the EFC of the PhC.[10] We have observed that this angle is indeed slightly higher (about 37°) than that predicted using the value obtained from the FDTD simulations. This deviation could be originated from the variation of the field penetration (generalized Goos-Hänchen effect discussed above) with the angle of incidence. Figure 4(f) shows the magnetic field distribution for $\phi_i=37°$, in which total external reflection can be observed.

It should be noted that ϕ_r is roughly estimated from the Gaussian waves traveling through free-space before and after the PhC slab so the lateral shift d in Fig. 2(a) can be obtained. It is difficult to obtain ϕ_r from the beam propagation inside the PhC because of the internal reflections at the air-PhC interfaces and the finiteness of the computational domain, which makes difficult to observe single beam propagation inside the PhC. The direction of the beam inside the PhC can be observed at early time steps of the FDTD simulations when reflections at the output interface are not yet well developed. This fact can be observed in Figs. 7(a), 7(b), 7(c), and 7(d) that show the magnetic field distribution at four different time steps, 150, 300, 450, and 600, respectively, expressed in units of ct/a, t being absolute time, for $fa/c=0.33$ and $\phi_i=17.5°$. In Fig. 7(a) the beam has not reached the output interface and the distance d cannot be correctly estimated as only a small part of the beam is out of the slab. However, the direction of propagation of the beam is well defined and is in good agreement with the value obtained from d in Fig. 4(d). In Fig. 7(b) the beam has fully reached the output interface: the refracted beam outside the slab has a well defined direction and the shift d can be estimated to obtain ϕ_r. The outer beam keeps almost the same for higher time steps [see Figs. 7(c) and 7(d)] so the same value of d would be obtained. However, owing to the reflection at the output interface and the finite extension of the slab in the transverse direction the field distribution inside the slab becomes highly complicated for long simulation times and large incident angles. In none of these figures the steady state has been reached, but ϕ_r can be estimated from the beam outside the slab and estimating the shift d. It should be mentioned that to reach the steady state by means of FDTD simulations becomes very difficult since the simulation time can be very large. This issue is beyond the scope of this paper and we consider that the obtained ϕ_r is a good approach to its real value. We assume that for $ct/a=300$ the refracted wave out of the PhC slab has reached its definitive direction so the distance d and, consequently, the angle ϕ_r can be estimated. For example, magnetic field distributions in Figs. 4 and 9–11 and results in Figs. 5 and 6 are obtained at a time step of $ct/a=300$. It should be also mentioned that if the simulation time is too large, beams originated from multiple reflections inside the PhC can exit the slab and modify the external beam that is used to obtain d. This oc-

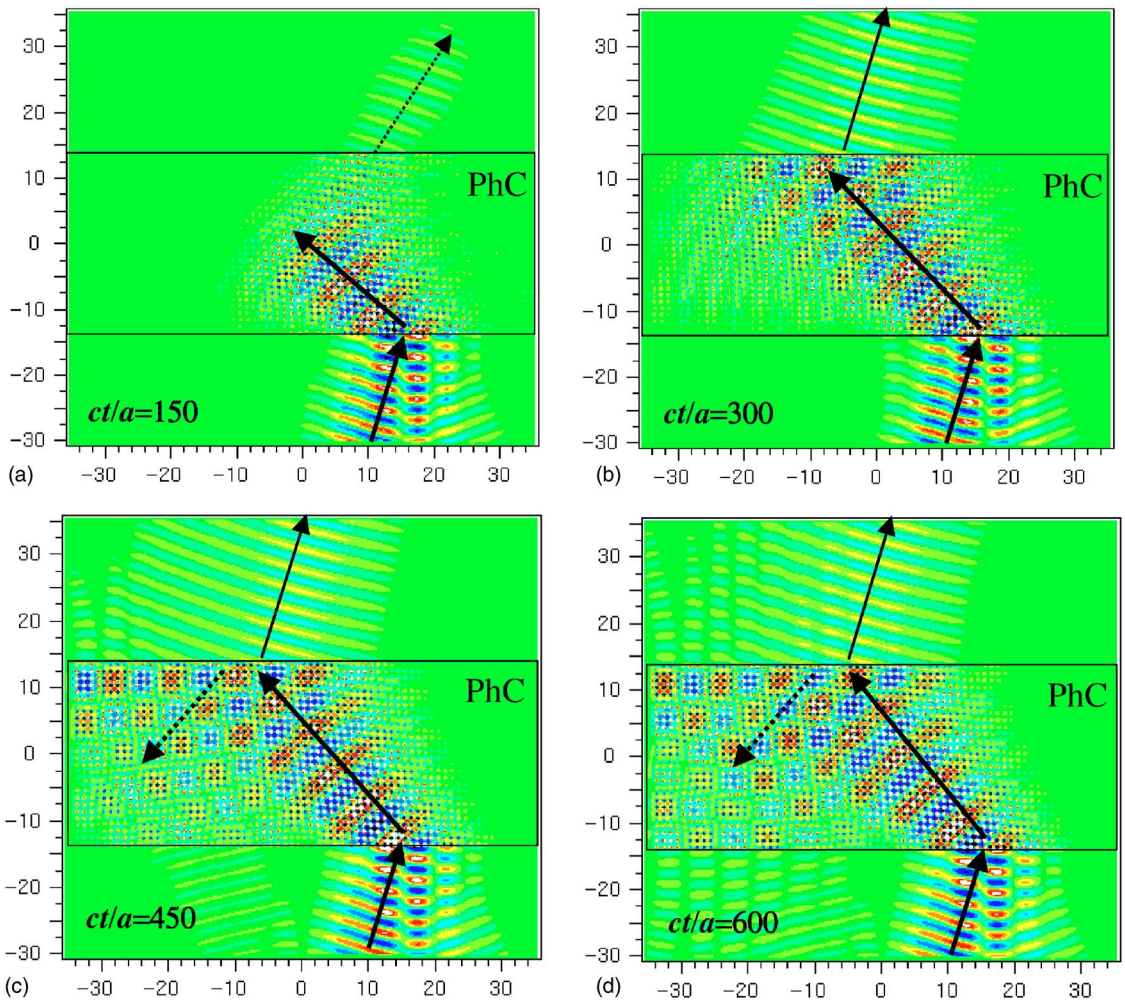

FIG. 7. (Color online) Distribution of the magnetic field parallel to the rods (FDTD simulations) taken at different time steps: $ct/a=150$ (a), 300 (b), 450 (c), and 600 (d). Parameters: $\phi_i=17.5°$ and $fa/c=0.33$. The width of the input beam is $15a$. Arrows highlight the direction of the energy of the incident wave, the wave inside the slab and the output wave. Red, green, and blue colors stand for positive, zero, and negative amplitude of the propagating field.

curs when L is modified to characterize the Goos-Hänchen effect and should be carefully taken into account mainly for small values of L.

B. PhC slab with orientation 2

Next we analyze wave propagation for orientation 2 [see Fig. 2(c)]. If the interface is kept horizontal, the lattice as well as the reciprocal space have to be rotated 45° (as depicted in Fig. 8, in which the rotation is rightwards) in order to have a termination along ΓM. In this case the periodicity of the interface is $P=\sqrt{2}a$, so the vertical lines that define the wave vectors excited inside the PhC are spaced $2\pi/\sqrt{2}a$. As in the case of orientation 1, for the nine reciprocal unit cells depicted nine wave vectors that do not violate causality are defined, and again, these wave vectors are related to the reciprocal space wave vectors by the relation $\vec{k}_{m,n}=\vec{k}_0+m\vec{G}_x+n\vec{G}_y$, for m, $n=-1$, 0, and 1. This means that all these wave vectors form part of a unique Bloch mode whose group velocity is given by the dashed arrow in Fig. 8. In principle, it seems that the situation is the same that for orientation 1 (the fundamental wave vector $\vec{k}_0$ is the same for both orientations), so the EM wave should propagate inside PhC resembling a negative refraction behavior. However, FDTD simulations shown in Fig. 9 reveal a well different behavior. Figure 9(a) represents the magnetic field distribution for $fa/c=0.33$ and normal incidence. The thickness of the slab is $L=20\sqrt{2}a$. The interface terminations are as depicted in Fig. 2(c). We observe that the field amplitude is very weak inside the slab and radiation outside the PhC slab is not observed. This can be explained by considering that the second photonic band for wave vectors along ΓX is an uncoupled state that is antisymmetric with respect to the input plane wave so the field inside the PhC cannot be excited in an efficient way.[19] We have estimated both the transmittance and reflectance for normal incidence in the case of orientation 2 and the result is that the transmittance is on the order of 10^{-4} whilst the reflectance power is close to unit. This is in clear contrast with the same measurements for orientation 1, for which the transmittance is about 0.8 and the reflectance about 0.2. Similar results were obtained for other frequencies

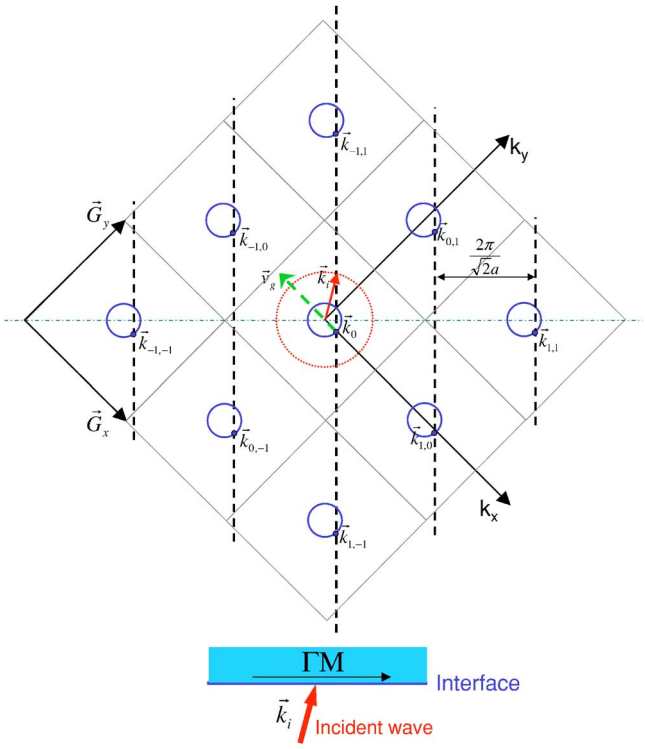

FIG. 8. (Color online) EFC diagram of refraction at the air-PhC interface for orientation 2 and $fa/c=0.33$. Nine reciprocal unit cells are shown. Blue solid and red dotted circles stand for the EFCs inside the PhC and in air, respectively. Vertical dashed lines (spaced $2\pi/\sqrt{2}a$) represent the conservation of the parallel component of the wave vectors. The wave vector of the incident waves is given by $\vec{k}_i$. The propagation direction inside the PhC is given by $\vec{v}_g$ (green dashed arrow). Bottom: scheme of the interface for orientation 2.

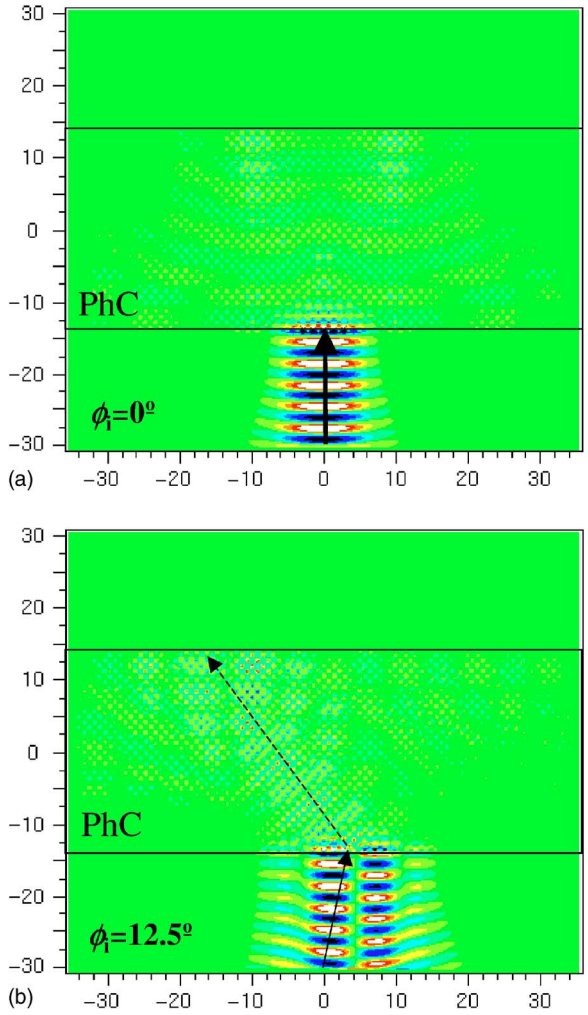

FIG. 9. (Color online) Distribution of the magnetic field parallel to the rods (FDTD simulations) for orientation 2 and $fa/c=0.33$. The incident angle ϕ_i is highlighted in each snapshot. The boundaries of the PhC slab are defined by the rectangle. The width of the input beam is $15a$. Arrows highlight the direction of the energy of the incident wave and the wave inside the slab. Red, green, and blue colors stand for positive, zero, and negative amplitude of the propagating field. The snapshots have been obtained after a simulation time of $ct/a=300$.

corresponding to the second photonic band. We checked this observation by calculating the transmission spectrum for normal incidence and the result was a very poor transmittance over the whole second band. This behavior was previously observed experimentally in a hexagonal PhC of dielectric rods in air at frequencies corresponding to the fifth photonic band and also in a negative n_{eff} regime.[10] Figure 9(b) shows the same magnetic field distribution for $\phi_i=12.5°$. Surprisingly we find that the coupling from the external plane wave to the field inside the PhC is more efficient than for normal incidence. This behavior, which also was observed for other incident angles around 12.5°, can be explained by considering that when the angle of incidence is modified the coupling efficiency that depends on the symmetry of the air and the PhC modes is also modified, and can be stronger for incident angles higher than 0°. In the case of $\phi_i=12.5°$ a shallow beam can be seen inside the PhC slab but it is not possible to determine accurately the refracted angle because the beam is diffuse. However, it seems that the beam propagates mainly in the negative direction, as predicted from the EFC analysis. For incident angles higher than 12.5°, the propagating beam inside the PhC slab was even weaker. We can conclude that owing to the poor coupling efficiency, the PhC with orientation 2 cannot be considered as an effective medium as previously observed for orientation 1.

C. PhC slab with orientation 3

In this case [see Fig. 2(d)] the periodicity of the interface is $P=\sqrt{5}a$ so condition (2) applied to the EFC diagram results in a set of parallel lines normal to the interface and spaced $2\pi/\sqrt{5}a$. The EFC analysis is similar to that for orientations 1 and 2 shown in Figs. 3 and 8 and is not reproduced here for the sake of simplicity. Once more, all the possible wave vectors obtained from the intersections between the vertical parallel lines (2) and the PhC EFCs accomplish the condition $\vec{k}_{m,n}=\vec{k}_0+m\vec{G}_x+n\vec{G}_y$, for m, $n=-1$, 0, and 1, so a unique Bloch mode is excited. In general, this behavior can be extended for any orientation for which the resulting interface is periodic. The propagation direction would be also in the negative direction as the PhC EFC inside the first Brillouin zone and the fundamental wave vec-

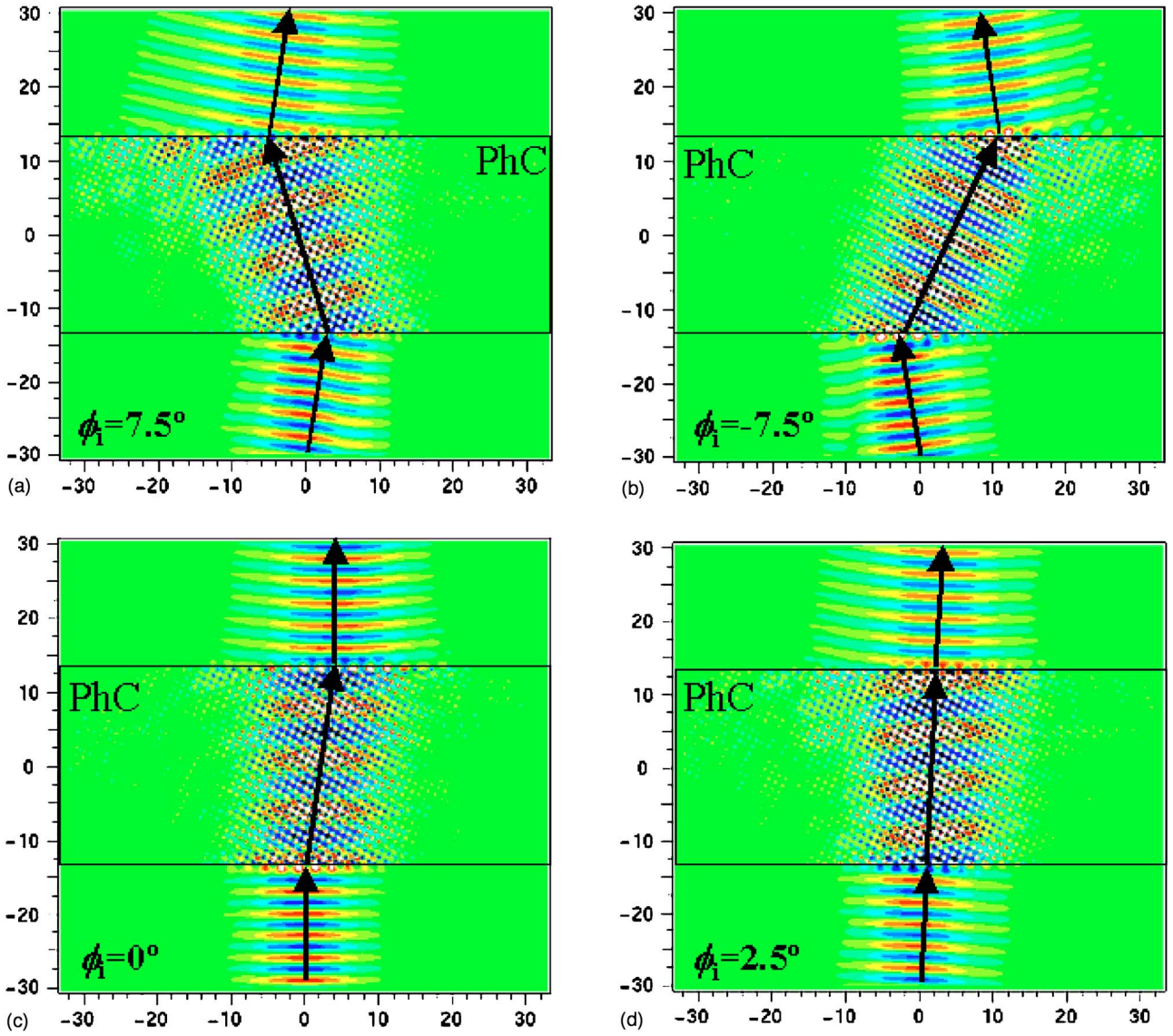

FIG. 10. (Color online) Distribution of the magnetic field parallel to the rods (FDTD simulations) for orientation 3. The incident angle ϕ_i is highlighted in each snapshot. The boundaries of the PhC slab are defined by the rectangle. The width of the input beam is $15a$. Arrows highlight the direction of the energy of the incident wave, the wave inside the slab, and the output wave. Red, green, and blue colors stand for positive, zero, and negative amplitude of the propagating field. The snapshots have been obtained after a simulation time of $ct/a=300$.

tor $\vec{k}_0$ are the same that for orientations 1 and 2. The only question that remains unsolved is if the coupling efficiency inside the PhC will be high as for orientation 1 or poor as in the case of orientation 2. To this end, FDTD simulations are carried out. The slab thickness for this case is $L=12\sqrt{5}a$ in order to ensure that the input and output interfaces are identical as depicted in Fig. 2(d). Figure 10(a) shows the magnetic field distribution when the incident angle is $\phi_i=7.5°$. A high coupling efficiency is observed and the beam propagates inside the PhC slab as in the case of orientation 1. In this case, estimated values of the transmittance and reflectance for normal incidence are 0.98 and 0.02, respectively, so the performance (in the sense of coupling efficiency) for orientation 3 is even better than for orientation 1. Negative refraction is observed at both interfaces. The estimated value of ϕ_r is 14°, which corresponds to $n_{eff}=-0.54$. This is in good agreement with the value obtained for the refractive index in the case of orientation 1. However, if the incident wave is launched with a negative ϕ_i we observe an interesting behavior. For example, Fig. 10(b) is similar to Fig. 10(a) but the incidence is from right to left ($\phi_i=-7.5°$). We observe that negative refraction also occurs at both interfaces but, in this case, the refracted angle is $\phi_r=25°$ so the corresponding refractive index is $n_{eff}=-0.3$. This asymmetry has its origin in the shape of the EFC at the frequency under consideration ($fa/c=0.33$), which is not completely rounded but it preserves a squarelike shape. This results in a variation of n_{eff} with the angle of incidence, which is an effect that does not occur in an effective medium. The effect is even more pronounced for small incident angles. For example, Fig. 10(c) shows the magnetic field distribution for normal incidence ($\phi_i=0°$). It can be observed that the beam is de-

flected rightwards with $\phi_r=9°$. If the Snell's law was applied to this case an infinite value of n_{eff} would result. For $\phi_i=2.5°$, as depicted in Fig. 10(d), the beam crosses the PhC slab without altering its direction ($\phi_r=2.5°$) so a value of $n_{eff}=1$ can be associated to this direction of incidence. We can state that the PhC does not behave as an effective refractive medium for this orientation since the effective index strongly depends on the direction of incidence.[13] This behavior could be alleviated by increasing the frequency so the EFCs get more rounded. However, this would also result in a lower coupling efficiency because the group velocity of the Bloch mode would tend to zero when approaching to the band gap lower edge ($fa/c=0.34$). In conclusion, although the beam is negative deflected for this orientation, the PhC does not behave as a true effective refractive medium.

D. PhC slab with orientation 4

Finally, we consider orientation 4 [see Fig. 2(e)]. The rotation angle of the lattice has been chosen to ensure that the interface is not periodic regardless of the slab thickness. We can assume that the PhC termination has an infinite periodicity P. Since the impinging external beam is finite in the transversal direction, the beam does not "see" any periodicity when reaches the interface. If we apply condition (2) to construct the vertical lines that were used previously in Figs. 3 and 8 to predict the direction of the refracted beam, we would obtain infinite intersection points in each EFC since the spacing between vertical lines would tend to zero. But, in this case, the wave vectors of the intersection points would not accomplish the relationship $\vec{k}_{m,n}=\vec{k}_0+m\vec{G}_x+n\vec{G}_y$, for m, $n=-1$, 0, and 1, so infinite waves (corresponding to a same Bloch mode but with different wave vectors and, consequently, different propagation directions) would be excited in principle. However, we are unable to predict which ones of them would carry the main part of the EM energy in order to determine the main propagation direction. Thus, the behavior of the system for orientation 4 will be studied only by means of FDTD simulations. Figures 11(a), 11(b), and 11(c) show the magnetic field distribution for orientation 4, $fa/c=0.33$ and incident angles $\phi_i=0°$, 12.5°, and −12.5°, respectively. For normal incidence [Fig. 11(a)] propagation inside the PhC is highly diffuse and it seems to be originated from diffraction at the input interface. A single well-definite beam is not observed inside the PhC. Instead, three shallow diffracted beams are observed. It is clear that the PhC does not show a refractive behavior. When $\phi_i=12.5°$ a main positively deflected diffracted beam is observed inside the PhC slab. There is also a shallow beam that is negatively deflected. A similar behavior was observed for other values of $\phi_i>0$. Finally, when $\phi_i=-12.5°$ a unique shallow beam that is negatively deflected is observed inside the PhC. Surprisingly, the direction of the main deflected beam inside the PhC is the same for both $\phi_i=12.5°$ and −12.5°, but the behavior cannot be considered refractive in any case. It is also interesting the presence of a strong high-order reflected beam in Fig. 11(c). It should be noted that we found a similar behavior for other nonperiodic slab terminations. We can conclude that the nonperiodicity of the interface avoids a refractive behavior of the PhC.

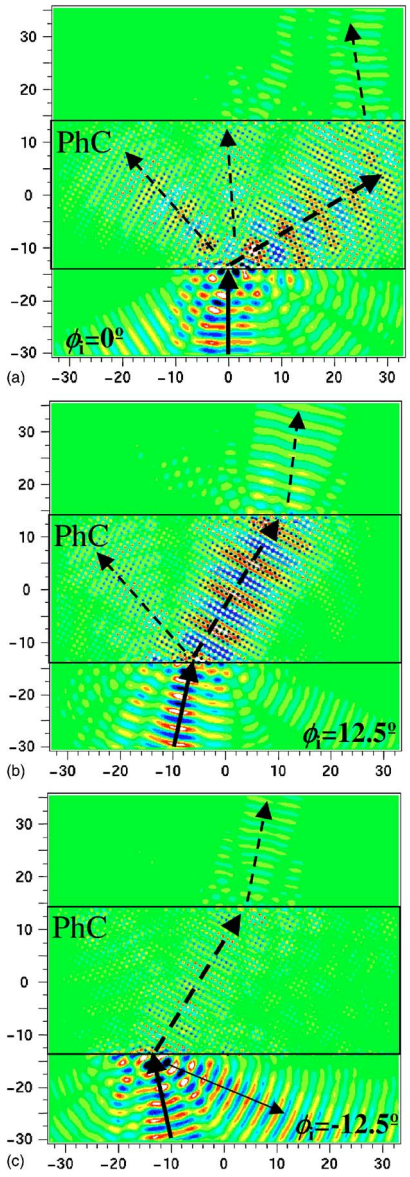

FIG. 11. (Color online) Distribution of the magnetic field parallel to the rods (FDTD simulations) for orientation 4. The incident angle ϕ_i is highlighted in each snapshot. The boundaries of the PhC slab are defined by the rectangle. The width of the input beam is $15a$. Bold solid arrows highlight the direction of the energy of the incident wave. The directions of the main diffracted beams are given by the dashed arrows. The thin solid arrow in (c) highlights the direction of a strong high-order reflected beam. Red, green, and blue colors stand for positive, zero, and negative amplitude of the propagating field. The snapshots have been obtained after a simulation time of $ct/a=300$.

IV. DISCUSSION: EFFECT ON THE FOCUSING PROPERTIES

The results shown in Sec. III lead us to conclude that the rounded shape of the EFC along with the decrease of the EFC radius with frequency are not sufficient to guarantee a negative refractive behavior of a PhC at a given frequency. If the PhC is not periodic (case of orientation 4) the propagation of the EM radiation inside the PhC has a clear diffrac-

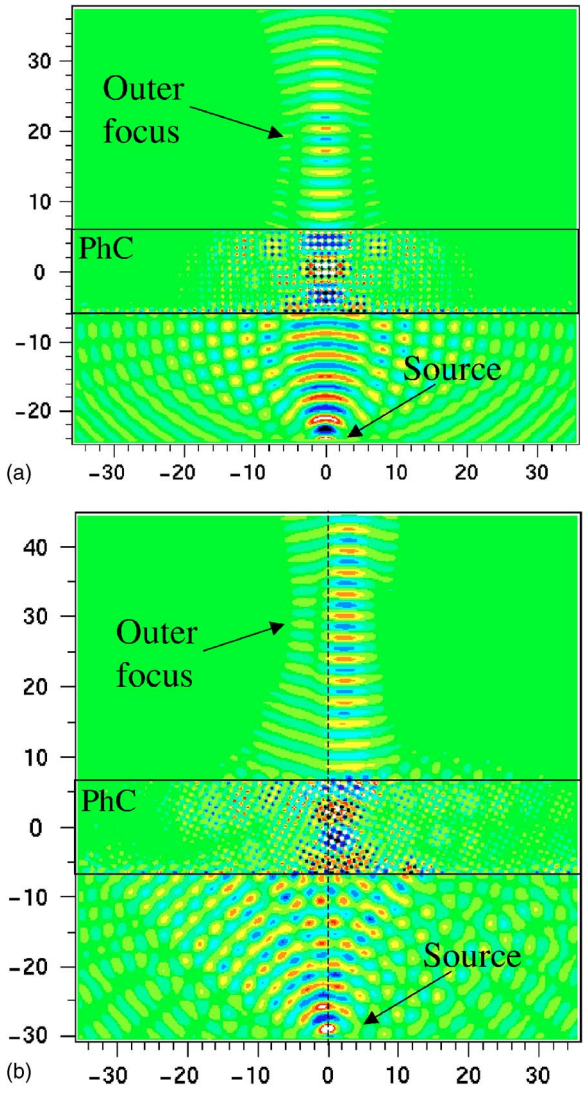

FIG. 12. (Color online) Distribution of the magnetic field parallel to the holes (FDTD simulations) for the PhC slab lens. The source has a Gaussian transverse profile with an initial width of 0.25λ. (a) orientation 1, $L=12a$; (b) orientation 3, $L=6\sqrt{5}a$. The positions of the source and the outer focus are indicated.

tive behavior that cannot be predicted from a EFC analysis. If the interface is periodic, a single Bloch mode is excited inside the PhC assuming a good coupling efficiency from an external plane wave, which is not accomplished for orientation 2. A refractive behavior is observed for periodic interfaces for which the EM waves at both sides of the interface are symmetry matched, which occurs for orientations 1 and 3. However, for orientation 3 the residual squarelike shape of the EFC inherited from the contour of the first Brillouin zone still has an important influence on the wave propagation and the Snell's law is not satisfied. To analyze more in depth this effect, we will study the focusing phenomenon by a flat slab[11,12] and both orientations 1 and 3.

FDTD simulations have been carried out to analyze the focusing behavior. Figures 12(a) and 12(b) show the magnetic field distribution for orientations 1 and 3, respectively. The slab thickness is $L=12a$ for orientation 1 and $L=6\sqrt{5}a$ for orientation 3. The optical source is a Gaussian beam with the frequency is $fa/c=0.33$ and an initial waist of $\lambda/4$. An outer focus characterized by the narrowing of the output beam and the negative curvature of the magnetic field before reaching the narrowest beam region can be observed for orientation 1. The output beam is narrower than the input beam because not all the incident angles (wave vectors) of the Gaussian input wave can propagate inside the PhC, as seen in Sec. III. An inner focus is not observed but we think that this can be caused by the multiple reflections at the interfaces air-PhC because a narrowing of the beam after the PhC input interface is observed at early stages of the FDTD simulations.[10] Subwavelength focusing is not observed because only EM waves with incident angles higher than 37° are transmitted through the PhC slab. This limits the wave vector components (both propagating and evanescent) that can be recovered at the image plane so the resolution cannot be smaller than the wavelength. However, if the PhC slab is designed with surface termination as in orientation 1 and $n_{\text{eff}}=-1$ (all the wave vectors can be retained at the PhC slab exit), subwavelength focusing becomes feasible.[21] For orientation 3, focusing is also observed [see Fig. 12(b)] but there are some differences regarding the case of orientation 1. First, the output beam is not aligned with the line that contains the source and is normal to the interface [vertical dashed line in Fig. 12(b)]. This can be explained by considering that for normal incidence the beam is deviated inside the PhC, as shown in Fig. 10(c), due to the remaining squarelike shape of the EFC. This is also the reason to explain the antisymmetric of the transverse profile of the output beam. In addition, it can be appreciated that the focus in the longitudinal direction is very elongated for orientation 3. We can conclude that only for orientation 1 a good focusing behavior can be achieved whereas for orientation 3 a focusing can also be observed but since the Snell's law is not satisfied at interfaces the outer focus is distorted. This demonstrates that the lattice orientation as well as the slab termination have also a key influence on the focusing properties of a PhC.

V. CONCLUSION

Negative refraction at the interface between air and a 2D square PhC at frequencies corresponding to the second photonic band has been analyzed by means of EFC diagrams and FDTD simulations. Several lattice orientations inside the slab giving rise to different slab terminations have been considered to observe the influence of the lattice and the termination over the propagation of EM waves. In principle, from the EFC analysis it could be established that, if the EFC has a rounded shape and its radius decreases with frequency, the PhC should behave as a refractive medium with an effective index that, in this case, should be negative. However, we have found that these conditions are not sufficient for the PhC to behave as a negative refractive medium. EM propagation inside the PhC is highly sensitive to the lattice orientation and the interface periodicity. It can be stated that a negative refractionlike behavior can only be observed when the interface is periodic and the mode symmetries of the external plane wave and the Bloch wave inside the PhC are

matched. Even under this assumption, the Snell's law is not satisfied if the interface is not properly selected because the EFC retains a slight squarelike shape even for frequencies near the band gap. In addition, when the Snell's law is accomplished the finiteness of the PhC has an important effect and the Goos-Hänchen effect at the interfaces has to be considered to obtain the effective index of refraction. In summary, it can be established that negative refraction occurs under certain conditions but PhCs cannot be considered as an effective refractive medium because EM propagation is sensitive to the lattice orientation and the slab termination.

ACKNOWLEDGMENT

This work has been partially funded by the Spanish Ministry of Science and Technology under Grant No. TIC2002-01553.

*Email address: almarab@ntc.upv.es

[1] E. Yablonovitch, Phys. Rev. Lett. **58**, 2059 (1987).
[2] S. John, Phys. Rev. Lett. **58**, 2486 (1987).
[3] M. Notomi, Phys. Rev. B **62**, 10696 (2000).
[4] H. Kosaka, T. Kawashima, A. Tomita, M. Notomi, T. Tamamura, T. Sato, and S. Kawakami, Phys. Rev. B **58**, R10096 (1998).
[5] B. Gralak, S. Enoch, and G. Tayeb, J. Opt. Soc. Am. A **17**, 1012 (2000).
[6] E. Cubukcu, K. Aydin, E. Ozbay, S. Foteinopoulou, and C. M. Soukoulis, Nature (London) **423**, 604 (2003).
[7] S. Foteinopoulou and C. M. Soukoulis, Phys. Rev. B **67**, 235107 (2003).
[8] C. Luo, S. G. Johnson, J. D. Joannopoulos, and J. B. Pendry, Phys. Rev. B **65**, 201104(R) (2002).
[9] M. Qiu, L. Thylén, M. Swillo, and B. Jaskorzynska, IEEE J. Sel. Top. Quantum Electron. **9**, 106 (2003).
[10] A. Martínez, H. Míguez, A. Griol, and J. Martí, Phys. Rev. B **69**, 165119 (2004).
[11] V. G. Veselago, Sov. Phys. Usp. **10**, 509 (1968).
[12] J. B. Pendry, Phys. Rev. Lett. **85**, 3966 (2000).
[13] C.-H. Kuo and Z. Ye, Phys. Rev. E **70**, 026608 (2004).
[14] Hung-Ta Chien, Hui-Ting Tang, Chao-Hsien Kuo, Chii-Chang Chen, and Zhen Ye, Phys. Rev. B **70**, 113101 (2004).
[15] D. N. Chigrin, S. Enoch, C. M. Sotomayor Torres, and G. Tayeb, Opt. Express **11**, 1203 (2003).
[16] A. Taflove, *Computational Electrodynamics—The Finite Difference Time-Domain Method* (Artech-House, Boston, 1995); K. S. Yee, IEEE Trans. Antennas Propag. **14**, 302 (1966).
[17] J. P. Berenger, J. Comput. Phys. **114**, 185 (1994).
[18] Depending on the frequency region under consideration more than one Bloch mode can be excited. However, for the whole second photonic band there is a unique Bloch mode that can be excited by an external source.
[19] K. Sakoda, *Optical Properties of Photonic Crystals* (Springer, Berlin, 2001).
[20] D. Felbacq and R. Smaâli, Phys. Rev. Lett. **92**, 193902 (2004).
[21] X. Wang, Z. F. Ren, and K. Kempa, Opt. Express **12**, 2919 (2004).